processes

MDPI

Article

Toxic Anionic Azo Dye Removal from Artificial Wastewater by Using Polyaniline/Clay Nanocomposite Adsorbent: Isotherm, Kinetics and Thermodynamic Study

Mohammad Ilyas Khan [1,*], Saif Ahmed Yahya [1], Abubakr ElKhaleefa [1], Ihab Shigidi [1], Ismat Hassan Ali [2], Mohammad Rehan [3] and Abdul Majeed Pirzada [4]

[1] Department of Chemical Engineering, College of Engineering, King Khalid University, Abha 62529, Saudi Arabia; en.saifahmed@gmail.com (S.A.Y.); amelkhalee@kku.edu.sa (A.E.); etaha@kku.edu.sa (I.S.)
[2] Department of Chemistry, College of Science, King Khalid University, Abha 62529, Saudi Arabia; ihali@kku.edu.sa
[3] Center of Excellence in Environmental Studies (CEES), King Abdulaziz University, Jeddah 21589, Saudi Arabia; dr.mohammad_rehan@yahoo.co.uk
[4] Department of Environmental Sciences, Sindh Madressatul Islam University, Karachi 74000, Pakistan; ampirzada@smiu.edu.pk
* Correspondence: mkaan@kku.edu.sa

Abstract: This study presents the synthesis and utilization of a conductive polymer/clay nanocomposite for the adsorptive removal of an azo dye, methyl orange (MO), from artificial wastewater. The PANI-CLAY nanocomposites were synthesized by means of the oxidative polymerization route and characterized using the Brunauer, Emmett and Teller thermogravimetric analysis, Fourier-Transform Infrared spectra and Scanning Electron Microscopy. The surface area of the clay mineral decreased from 37.38 to 13.44 m^2/g for 10 g of PANI/CLAY when made into a composite with PANI. Such behavior is most likely due to the possible coverage of the clay surface by a layer of PANI. Further, TGA revealed that incorporating CLAY significantly improved the thermal stability of PANI. The effects of adsorption process parameters such as adsorbent dosage (0.006–0.4 g), solution pH (1, 3, 5, 7, 9, 11 and 13), initial dye concentration (50–300 ppm), contact time (1–80 min) and temperature (25 °C, 30 °C, 35 °C and 40 °C) on the % removal efficiency were investigated. The experimental data were well fitted by the pseudo-second-order kinetic model. The maximum uptake capacity (q_{max}) values increased from 42.017 mg/g (PANI/CLAY 10 g) to 55.87 mg/g for PANI alone. The uptake capacity implies that the prepared adsorbents possess excellent adsorption characteristics with high affinity towards organic dye removal.

Keywords: MO adsorption; wastewater; polyaniline/clay nanocomposite; isotherm models; kinetic models; thermodynamic study

check for updates

Academic Editors: Marwa El-Azazy, Saeed Al-Meer, Ahmed El-Shafie and Khalid Al-Saad

Received: 12 February 2025
Revised: 8 March 2025
Accepted: 10 March 2025
Published: 12 March 2025

Citation: Khan, M.I.; Yahya, S.A.; ElKhaleefa, A.; Shigidi, I.; Ali, I.H.; Rehan, M.; Pirzada, A.M. Toxic Anionic Azo Dye Removal from Artificial Wastewater by Using Polyaniline/Clay Nanocomposite Adsorbent: Isotherm, Kinetics and Thermodynamic Study. *Processes* **2025**, *13*, 827. https://doi.org/10.3390/pr13030827

Copyright: © 2025 by the authors. Licensee MDPI, Basel, Switzerland. This article is an open access article distributed under the terms and conditions of the Creative Commons Attribution (CC BY) license (https://creativecommons.org/licenses/by/4.0/).

1. Introduction

The industrial revolution introduced many organic dyes and colorants which are now widely used by a broad spectrum of industries. These include, for example, leather, textile, paper, cosmetics, pharmaceuticals, food processing and distillers. Based on the functional groups present in their chemical structures, organic dyes may be classified into different categories [1]. The major sources of organic dyes in industrial wastewater are textile manufacturing facilities and paint, paper and plastic processing industries [2,3]. The presence of organic dyes and colors in water bodies poses a significant threat to human health as well as the aquatic system owing to their carcinogenic and toxic nature [4]. This is

usually the result of undesirable colors blocking direct sunlight (photosynthesis process) as well as causing an indirect severe health risk, as proven in many researches [5]. As a result, several strict environmental and pollution control legislations were enacted by governments and decision-makers [6]. Due to the strict environmental legislation, scientists and engineers have been searching for feasible, cost-effective, environmentally friendly and effective methods for wastewater treatment technologies. These include chemical (flocculation/coagulation, advanced oxidation processes, ozonation, adsorption), physical (reverse osmosis and membrane technology, micro and nanofiltration) and biological treatment (aerobic and anaerobic digestion). Each one of these methods has their own advantages and disadvantages. For example, in the case of advanced oxidation processes, they consume energy and have running costs, while reverse osmosis and membrane technology, due to large pore sizes, is not applicable for wastewater treatment [7]. Adsorption when compared with other available techniques is the preferred choice. This is most likely due to its cost-effectiveness, simplicity, flexibility, ease of operation and control [8]. Adsorption can effectively be used for the remediation of various pollutants including organic dyes [9]. Different adsorbent materials are being reported in the literature for the removal of contaminants. These include activated carbon, silica gel, activated alumina, zeolites, polymers and resins, kaolin, soda ash, bentonite and carbon nanotubes (CNTs), as reported by [10]. Clay-based adsorbents have gained significant importance because they are non-toxic, highly available, inexpensive, chemically and mechanically stable and environmentally friendly, in addition to having a high surface area and advantageous structural properties [11]. Numerous clay-based minerals for water treatment have been reported in the literature [12,13]. To enhance the adsorption characteristics of adsorbents, various treatments/modifications can be applied. These include physical modifications (ultrasound, plasma, high-pressure homogenization, thermal heating, etc.), chemical modifications (acid/alkali, surfactant, silane coupling agent, surface grafting of polymer, etc.) and thermal modification [14–19]. The synthesis of conductive polymers with inorganic particles may impart significant changes (synergic or complementary behavior) to the properties of individual components of the composite [20,21]. Clay minerals modified with conductive polymers have enhanced adsorption characteristics due to the introduction of organic functional groups, their high cationic exchange capacity and sufficient active adsorption sites [22]. Among conductive polymers, the most commonly reported is polyaniline primarily because of its functional groups such as amine and imine. It is widely reported mostly due to its ease of synthesis, doping feasibility, physicochemical stability, environmental friendliness and monomer availability [23].

This work is a continuation of our previous work [24] in which the currently reported clay mineral was used without any modification for the adsorptive removal of methylene blue. The current investigation is an attempt to explore the adsorption potential of the same clay for removing the anionic dye methyl orange with surface modifications with polyaniline (PANI-CLAY composites) with different clay loadings (by weight). The motivation behind this work is to modify the clay with polyaniline and exploit the prepared composite as an adsorbent for MO removal. The effect of different process parameters on the % removal efficiency was explored and the optimum values for these parameters were thus applied to determine the maximum adsorption uptake capacity (q_{max}).

2. Materials and Methods

All the reagents and chemicals used in the current investigation were of analytical grade. All the chemicals were used as received. Aniline hydrochloride (99%), ammonium persulfate (98%) and the organic dye methyl orange (dye content 85%) were purchased from Sigma-Aldrich Chemie (GmbH, Taufkirchen, Germany). The clay mineral (also reported in

our earlier research [24]) was collected from the Southern region of Saudi Arabia. Sodium hydroxide (97%) 1M and hydrochloric acid (37%) were used for pH adjustment of the adsorbate solution.

In a 250 mL conical flask, aniline hydrochloride (purum; 5.18 g) was dissolved in distilled water to make 100 mL of solution. To make a 100 mL solution of ammonium persulfate, purum (11.42 g) was dissolved in distilled water. Both solutions were stirred and then kept in an ice bath at a temperature of ~0–3 °C for 1 h. Aniline hydrochloride solution was poured into a 250 mL beaker that was magnetically stirred, while ammonium persulfate was added drop-wise to the same beaker and stirring was continued for 2 h to achieve complete polymerization. The ice-cold reactants were polymerized at room temperature at 23.5 °C. A color change from light blue through bluish-black and finally to greenish-black was observed as the solutions polymerized. The contents were filtered and the solid residue (PANI) was collected on the filter paper and rinsed with 100 mL of distilled water three to four times followed by rinsing with 50 mL of acetone, as reported in [25–28]. The obtained residue was subjected to drying in a conventional oven for 24 h at 60 °C. The final product in powder form was obtained by grinding using a mortar and pestle.

A similar procedure was used to synthesize the PANI/clay composite. Aniline hydrochloride was dissolved in distilled water to make 100 mL of solution in a conical flask and 1 g of clay was dispersed in it. Ammonium persulfate was also dissolved in distilled water to make 100 mL of solution. The aniline hydrochloride/clay dispersion was kept in an ultrasonic ice bath at a temperature of ~0–3 °C for 2 h. Ammonium persulfate was stirred and kept in an ice bath at a temperature of ~0–3 °C for 2 h. Then, the aniline hydrochloride/clay solution was poured into a 250 mL beaker and ammonium persulfate was added to the same beaker drop-wise under magnetic stirring at 300 rpm for 2 h for the solutions to completely polymerize. After that, the contents were filtered and the solid residue (PANI/clay) was collected on filter paper and rinsed with 100 mL of distilled water three to four times followed by rinsing with 50 mL of acetone. The obtained residue was subjected to drying in a conventional oven for 24 h at 60 °C. The final product in powder form was obtained by grinding using a mortar and pestle. The same procedures were repeated with different clay loadings (5 g and 10 g).

In order to prepare the stock solution of 500 ppm MO solution, 0.5 g of methyl orange dye was dissolved in 1000 mL of distilled water and briefly stirred. The prepared stock solution was kept in a 1000 mL flat-bottomed flask for use in further experiments. From the stock solutions, further dilutions were made for the subsequent adsorption experiments.

To investigate the impact of different process parameters such as adsorbent dosage, pH, contact time, initial dye concentration and temperature, batch adsorption experiments were carried out. In each case, a known quantity of adsorbent was added to a known volume of the prepared dye-containing solution and mixed in a temperature-controlled shaker for a given period. At the end of each experiment, the mixed solutions were filtered using Whatman paper No 40 with a pore size of approximately 15 microns. The filtered solution was collected and analyzed for the residual dye concentration using a UV spectrophotometer with a wavelength of 465 nm [29,30]. The percentage (%) dye removal was determined using Equation (1), while using Equation (2), the equilibrium uptake capacity was calculated.

$$Removal\ (\%) = \frac{C_0 - C_e}{C_o} \times 100 \quad (1)$$

$$q_e = (C_o - C_e)V/W \quad (2)$$

where C_e = equilibrium concentration of dye (mg/L), C_o = initial dye concentration (mg/L) and q_e = adsorbent equilibrium uptake capacity. V and W are the solution volume (L) and adsorbent mass (g), respectively.

To investigate the effect of adsorbent dosage, 25 mL of 50 ppm MO solution was measured in sampling bottles. An adsorbent dosage of PANI ranging from 0.0005 g to 0.4 g was added to each sample bottle. Then, at 25 °C, the sample bottles containing the prepared solution and PANI were placed in a temperature-controlled shaker for 1 h at 120 rpm. Then, the samples were filtered and the filtrates were collected for UV analysis to determine the remaining residual concentration and the optimum dosage of adsorbent with the highest removal efficiency. The same procedures were repeated for each of the three PANI/CLAY composites with different (1 g, 5 g and 10 g) clay loadings but with 10 different amounts/dosages of PANI/CLAY ranging from 0.006 g to 0.4 g.

The pH zero-point charge, pH_{PZC}, refers to the pH at which the adsorbent surface has equal number of positive and negative charges, was determined by using the constant mass of adsorbent method. A 50 mL solution of sodium chloride (0.01 N) was added to a series of 100 mL beakers. The pH of the solution in these beakers was adjusted to obtain a range of solution pH. Following this step, a fixed amount of adsorbent (0.15 g) was introduced into each beaker and left undisturbed for 48 h. The final pH of the solution was then measured and plotted to determine the pH_{PZC} value. Solutions of various pH containing 50 ppm MO (100 mL) were prepared by pH adjustment using either 1 M NaOH or HCl solutions, and the prepared solutions were poured into 250 mL beakers. Finally, 6 samples of 100 mL of 50 ppm MO solutions with different pH values of 1, 3, 5, 7, 9, 11 and 13 were obtained. After that, to examine the impact of solution pH, 6 samples of 25 mL of the different pH solutions were measured into sampling bottles. To each sample bottle, 0.2 g of PANI was added as it was the optimal dosage. Then, at 25 °C, the sample bottles containing different pH solutions and PANI were placed in a temperature-controlled shaker for 1 h at 120 rpm. Then, the samples were filtered. The same procedures were repeated for each of the three PANI/CLAY composites of 1 g, 5 g and 10 g clay portions. After that, the filtrates were collected for UV spectrophotometric analysis to assess the remaining concentration of the dye so that the optimum pH values could be determined.

To investigate the impact of contact time, the MO solution pH was kept at a neutral value. Then, 7 samples of 25 mL of 50 ppm MO solution were measured into 7 sampling bottles. To each sample bottle, 0.2 g of PANI was added. Then, at 25 °C, the sample bottles were placed in a shaker that is temperature-controlled at 120 rpm. Each one of the 7 samples was removed from the shaker and filtered at different periods starting from 1 min up to 80 min. Again, the same procedures were repeated for each of the three PANI/CLAY composites of 1 g, 5 g and 10 g clay portions. After that, the filtrates were collected for UV analysis to determine the remaining residual concentration for optimum contact time determination.

To investigate the effect of initial dye concentration, 100 mL solutions of different MO dye concentrations (from 50 ppm to 300 ppm) were prepared. Then, 25 mL solutions were measured into sampling bottles and 0.2 g of the adsorbent was added to each sample bottle and subjected to shaking for 1 h in a shaker that is temperature-controlled at 120 rpm. The contents were filtered and collected for UV analysis to evaluate the residual dye concentrations. The same procedures were repeated for each of the prepared adsorbents.

To study the effect of temperature, 25 mL samples of 100 ppm MO solution were prepared and added to the sampling bottles. To each sample bottle, 0.2 g of the test composite was added. Then, the sample bottles were placed in a temperature-controlled shaker for 1 h at 120 rpm at different temperature intervals (25 °C, 30 °C, 35 °C and 40 °C). Then, the samples were filtered and the residue was collected and analyzed by using a UV spectrophotometer as discussed earlier.

3. Results and Discussion

3.1. Characterization

3.1.1. BET Analysis

Surface characteristics (pore size, surface area and pore volume) for PANI, PANI/CLAY 1 g, PANI/CLAY 5 g and PANI/CLAY 10 g were determined using NOVA 4200e surface area and pore size analyzer (Quantachrome Instruments, Boynton Beach, FL, USA). The obtained results are listed in Table 1. Furthermore, the adsorbed N_2 quantity on the prepared adsorbents is shown in Figure 1. The results of pore radius reveal a mesoporous structure since the average pore sizes are between 1 and 25 nm.

Table 1. Surface area data of Clay, PANI, PANI/CLAY 1 g, PANI/CLAY 5 g and PANI/CLAY 10 g.

Method	CLAY	PANI	PANI/CLAY 1 g	PANI/CLAY 5 g	PANI/CLAY 10 g
MultiPoint BET (m^2/g)	37.38	25.35	22.91	13.32	13.44
BJH method cumulative adsorption pore volume (cm^3/g)	0.0486	0.0295	0.0277	0.0195	0.0225
BJH method adsorption pore radius (Å)	17.41	19.56	18.32	18.34	18.17

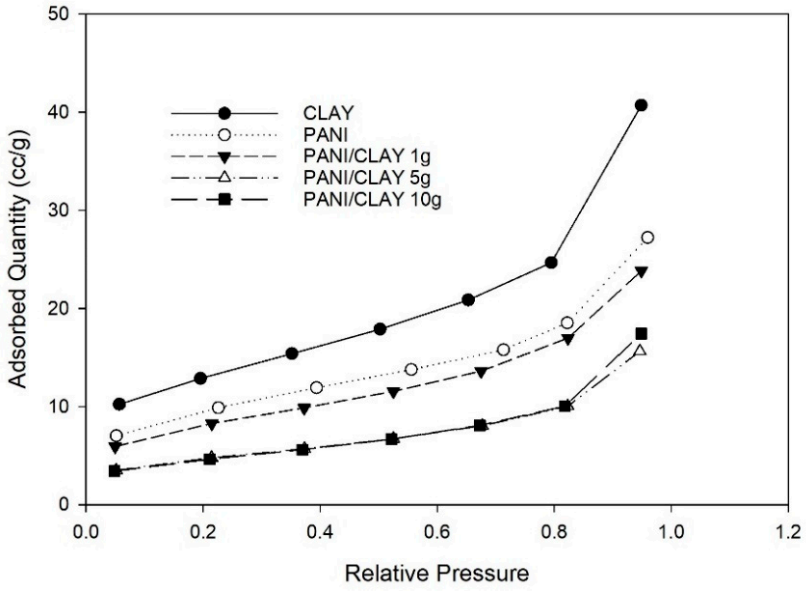


Figure 1. N_2 adsorption curves of clay, PANI, PANI/CLAY 1 g, PANI/CLAY 5 g and PANI/CLAY 10 g.

Furthermore, some differences were observed in the N_2 adsorbed quantity between the clay, PANI and PANI/CLAY nanocomposites as presented in Figure 1. The clay has a larger surface area and pore volume compared to PANI and the prepared PANI/CLAY nanocomposites. However, by making nanocomposites out of the two, a decreasing trend in surface area and pore volume is observed with an increase in clay loading. Similar observations were reported for polyaniline nanocomposites with MMT [31]. This is most likely due to the formation of a PANI coating layer on the clay surfaces. The obtained results of both PANI and the PANI/clay composite are identical to those reported by [32] in the literature.

3.1.2. Thermogravimetric Analysis (TGA)

TGA was carried out for all of the prepared samples to assess the thermal stability. TGA was performed using thermal analyzer (TG209 F1 libra, NETZSCH-Gerätebau GmbH,

Selb, Germany) over a temperature range of 100–600 °C. The weight losses observed for the neat clay and all composite samples are less than those observed for the PANI sample, as presented in Figure 2. Weight losses in the temperature range of 100–400 °C may be attributed to the elimination of the acid dopant molecule that is normally attached to the chain of PANI and other low-molecular-weight oligomers. In the higher temperature range from 300 to 500 °C, the reason for such weight loss may be due to the decomposition and breaking down of PANI molecular chains [28,33]. The addition of clay to the PANI matrix led to significant improvements in PANI thermal stability, and the total weight loss % decreased with the increase in clay content. Such improvement in thermal stability may be attributed to the chemical bonding of the clay particles with molecular chains of the polymer, as reported in [34]. Furthermore, the additional exfoliated layered silicates can significantly decrease mass loss during degradation, thus improving the polymer/clay composite's thermal stability [35]. Similar observations were reported by [36] for PANI/CNT composites.

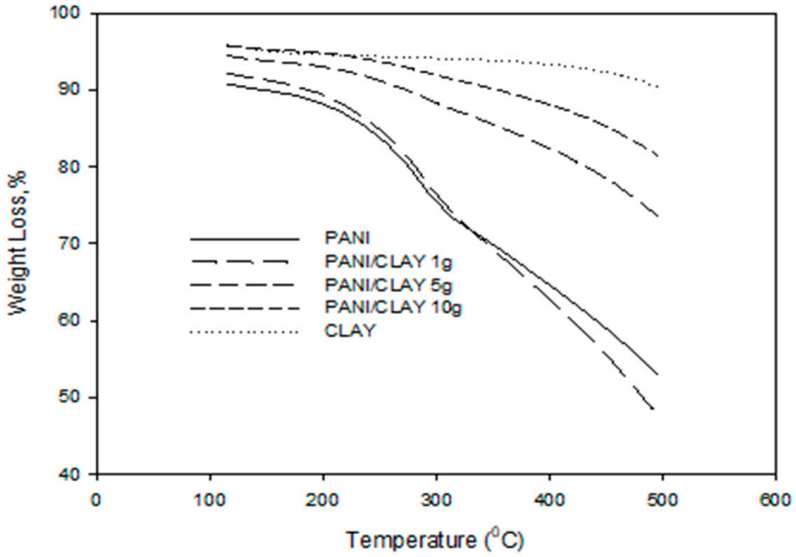


Figure 2. Thermogravimetric analysis.

3.1.3. IR Analysis

The infrared analysis (IR) was conducted using FTIR spectrometer (Agilent Cary 630, Agilent Technologies, Santa Clara, CA, USA) for the prepared samples to study the chemical structure of the adsorbents. The range of the spectrogram is between 4000 and 400 cm^{-1} and is presented in Figure 3. The characteristic bands corresponding to clay are 1000 cm^{-1} due to the stretching vibration of Si–O–Si in the clay matrix and 910 cm^{-1} due to the vibration in (Al–OH). Furthermore, the presence of moisture on the surface of free silica was identified from the IR peak observed at 1650 cm^{-1} [37]. Also, the corresponding bands at 3620 cm^{-1} and 3700 cm^{-1} are shown in the O–H stretching region because of Al–OH stretching vibrations. In the case of PANI and PANI/clay composites, the adsorption band at 1300 cm^{-1} can be attributed to the C-N stretching of secondary amines [38]. Also, the peaks ranging from 2100 to 2400 cm^{-1} are assigned to C≡C and C≡N. Furthermore, the peak at 2450 cm^{-1} corresponds to the vibration of N-H and unsaturated amine. Upon the addition of PANI to clay, the large peaks in the range of 500 to 1100 and 3600–3800 cm^{-1} in the clay IR spectra disappear, which is most likely due to the intercalation and coverage of the clay surface by PANI.

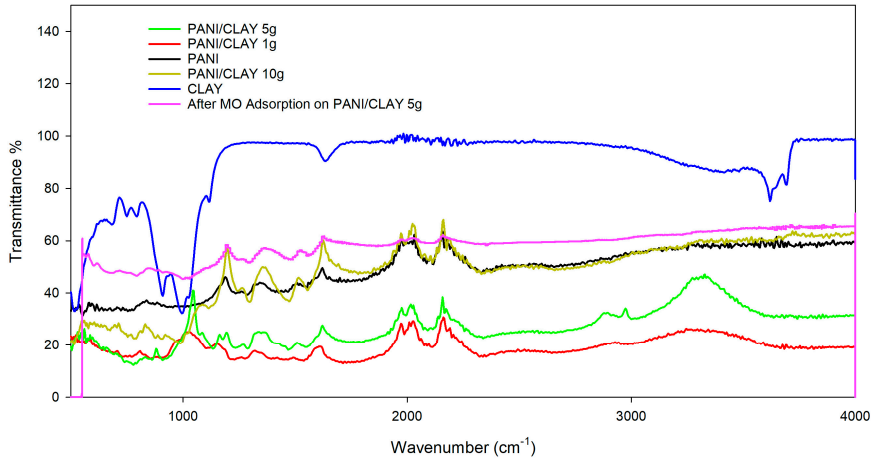


Figure 3. IR analysis of clay, PANI, PANI/CLAY 1 g, PANI/CLAY 5 g and PANI/CLAY 10 g, and after MO adsorption for PANI/CLAY 5 g.

3.1.4. SEM Analysis

The morphological characteristics of the clay and the prepared composite samples were evaluated with the help of Scanning Electron Microscopy (SEM), and the obtained results are displayed in Figure 4. The clay has an almost uniform porous structure compared to PANI, which is rod-like and clustered (Figure 4a,b). Mixing of the two components together (PANI and clay) led to particle agglomeration and the formation of microporous structures, as shown in Figure 4c–e.

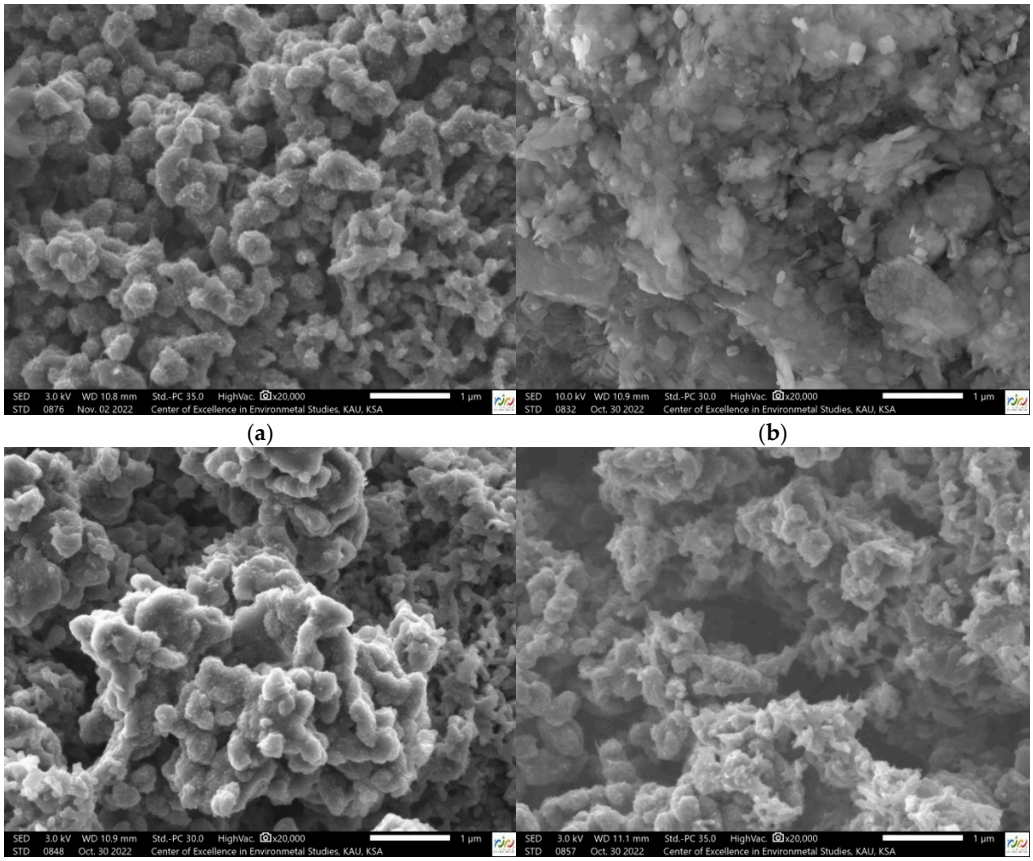
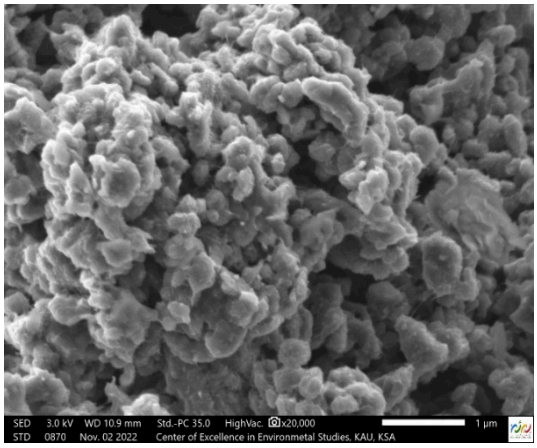


Figure 4. *Cont.*



(**e**)

Figure 4. SEM images of (**a**) clay, (**b**) PANI, (**c**) PANI/CLAY 1 g, (**d**) PANI/CLAY 5 g and (**e**) PANI/CLAY 10 g.

It can also be noted that the deposition of PANI within the clay voids, covering the clay surface, leads to a decrease in surface area and porosity. This is further confirmed by the BET analysis, the results of which are summarized in Table 1 and presented in Figure 1. Identical observations were reported by [39] for different clay/PANI composites and by [31] for MMT/PANI nanocomposites.

3.2. Adsorption Experiments

3.2.1. Effect of Adsorbent Dosage

The impact of the adsorbent dose on the % dye removal efficiency was investigated to determine the optimum adsorbent dosage value, which is crucial in terms of the availability of active binding sites and surface area for the adsorption process. Figure 5 depicts the impact of adsorbent amount on the MO % removal efficiency. The results show that removal efficiency and adsorption capacity have an inverse relationship with adsorbent dosage, as reported by [40]. This is probably due to active site saturation, particle agglomeration, clogging and possible reductions in surface area, in addition to the reduced driving force for mass transfer. The removal efficiency increased from 62% to 99% for PANI, from 61% to 99% for PANI/CLAY 1 g, from 31% to 99% for PANI/CLAY 5 g and from 26% to 99% for PANI/CLAY 10 g. As for the adsorption capacity, it decreased from 129.83 mg/g to 3.1 mg/g, from 129.05 mg/g to 2.75 mg/g, from 64.59 mg/g to 2.75 mg/g and from 53.62 mg/g to 2.74 mg/g in relation to the adsorbent dosage, respectively. Such behavior is expected because there is excess adsorbent (more available active sites) that the adsorbate molecules could possibly bind to. Similar behavior was reported by [41] for the removal of brilliant green using red clay, by [42] for the elimination of brilliant green and congo red by using polyaniline/clinoptilolite, by [43] for hazardous malachite green removal by using sepiolite and its adsorbents and by [44] for zinc oxide/polyaniline nanocomposite removal [45]. Furthermore, ref. [22] reported the use of clay/PANI/Fe_3O_4 to remove congo red, while an activated carbon–MMT composite was reported for the removal of crystal violet and methylene blue by [46]. The maximum dye removal efficiency was 99% for 0.45 g of the four composites with a constant dye concentration and solution volume of 50 ppm and 25 mL, respectively. Using only 0.2 g of adsorbent, further experiments were conducted, as a negligible effect beyond this weight was observed, as shown in Figure 5.

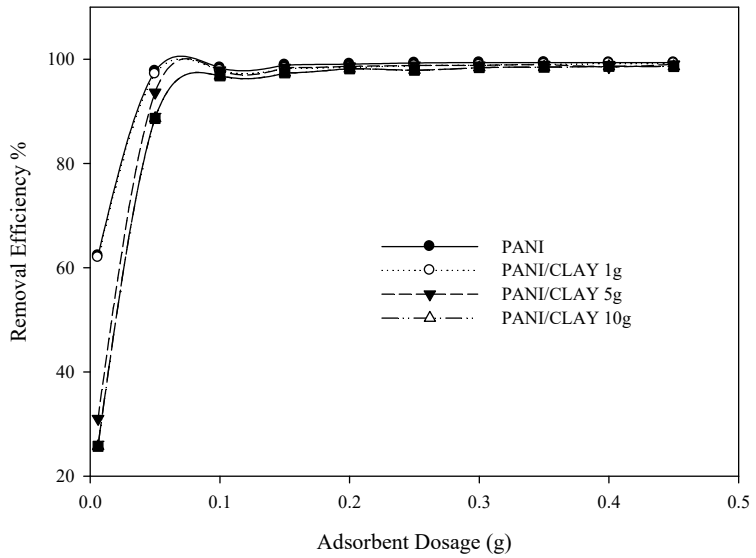


Figure 5. Effect of adsorbent dosage on removal efficiency of MO using PANI and its clay composites.

3.2.2. Effect of pH

Organic dye removal via the adsorption process is significantly affected by the pH of the solution. The removal % of anionic dye from aqueous media is usually high at low pH (acidic) mainly due to the electrostatic attraction between the negatively charged anionic dye and the positively charged adsorbent surfaces, in addition to the possible Van der Waals interactions, especially with very small pore sizes, which is usually the case when the pH is less than 5. For PANI and PANI/CLAY 1 g, the percentage removal efficiency almost remains constant throughout the studied range of pH, as shown in Figure 6a. However, for the composites with high clay contents, 5 g and 10 g, pH has a significant effect on the removal percentage. Under high acidic conditions, the % removal is low but increases when the pH reaches 5. No significant changes were noted in the range between 5 and 11 but a sharp reduction in the removal efficiency is observed between pH 11 and 13. In strongly acidic conditions, H^+ ions have a pivotal role in adsorbent/adsorbate interactions. However, in the very high pH range, OH^- competes with the adsorbate molecules to fill the active sites on the adsorbent surface, which results in lower % removal. Furthermore, the negative hydroxyl ions and anionic dye molecules cause electrostatic repulsion, which reduces the removal percentage. The zero-point charge (pH_{PZC}) value for our adsorbent was found to be 6.2, as shown in Figure 6b. In addition, from the colloidal chemical thermodynamical point of view, the tested adsorbent surface is expected to have a negative charge as long as $pH_{PZC} < pH$ and a positive charge when $pH_{PZC} > pH$ [47]. In a nutshell, it can be concluded that percentage removal is low at both ends of the pH range investigated. As a result, further experiments were conducted in near-neutral pH conditions.

Depending on the pH, PANI may exist either as the emeraldine salt or emeraldine base. The emeraldine salt forms in acidic conditions, while the emeraldine base normally forms in the base form. At neutral pH, the salt form of PANI may transform into the base form. On the other hand, the MO dye is known to be anionic (negatively charged), and PANI possesses a positive charge in the pH range of 5–8. Hence, the highest adsorption of MO was observed in this range, which is most likely due to the electrostatic forces of attraction. This point can be further explained by the net zero charge or point of zero charge (pH_{PZC}), which is 6.2 for PANI/CLAY 5 g, as shown in Figure 6b. Similar observations were reported by [38]. No significant changes in removal efficiency were observed in the alkaline pH range of $7 \leq pH \leq 11$. However, neutral pH appeared to be an ideal value

for further adsorption experiments due to the high removal efficiencies (99%) for PANI, PANI/CLAY 1 g, PANI/CLAY 5 g and (98%) for PANI/CLAY 10 g.

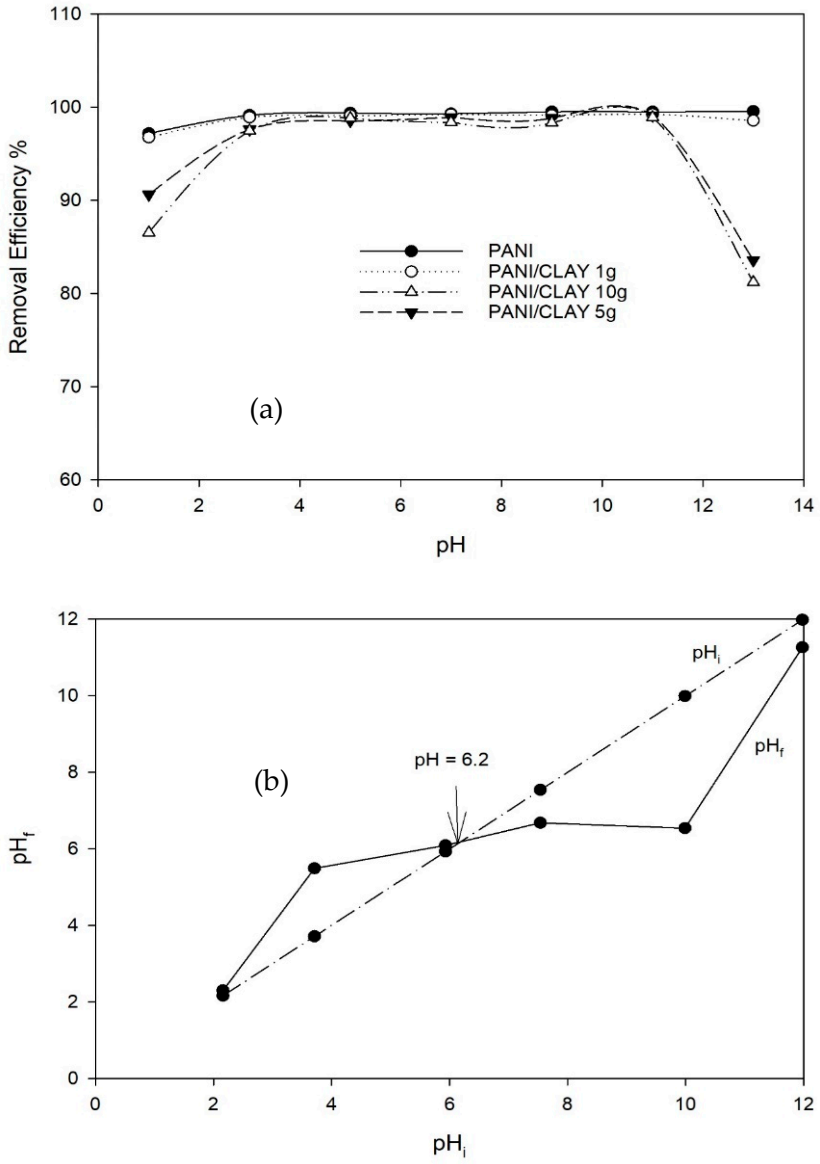


Figure 6. Effect of (**a**) solution pH and (**b**) pH_{PZC}.

3.2.3. Effect of Contact Time

Determination of the optimum contact time for adsorbent/adsorbate interactions and studying the adsorption kinetics are important. Thus, batch adsorbent experiments were conducted at a fixed adsorbent dosage (0.2 g) and a near-neutral pH (6.72). The only variable that was varied was the contact time in the range of 1–80 min. It was varied to determine the equilibrium time for the adsorption process. As shown in Figure 7, there is a rapid increase in the removal efficiency % (almost 98%) in the initial 40 min for all of the tested adsorbents, which may be attributed to the availability of surplus active sites on the adsorbent surface. No significant increase was observed between 40 and 80 min of contact time, which may be due to the exhaustion and occupation of almost all of the available active sites. Based on these results, a contact time of 60 min was selected for further experiments.

3.2.4. Effect of Initial Concentration

The impact of the initial dye concentration was assessed by having an incremental increase (50 ppm to 300 ppm) while keeping all other parameters constant. As expected, % removal efficiency decreased with increasing initial MO concentration, as shown in Figure 8. Again, such behavior is mostly due to the presence of a limited number of binding sites for adsorbent/adsorbate interactions. This intensifies the competition between the MO ions and the fixed number of active sites on the adsorbent surface resulting from a higher MO concentration (more adsorbate), which causes a reduction in the percentage removal of MO dye. Identical findings were reported by [9] for methylene blue dye removal by using nano glauconite clay.

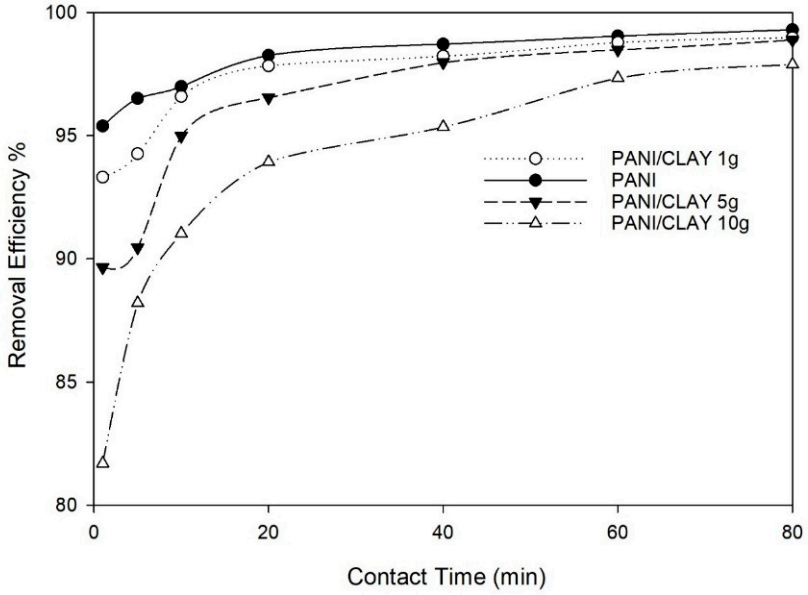


Figure 7. Variation in removal efficiency % of MO with respect to mixing time.

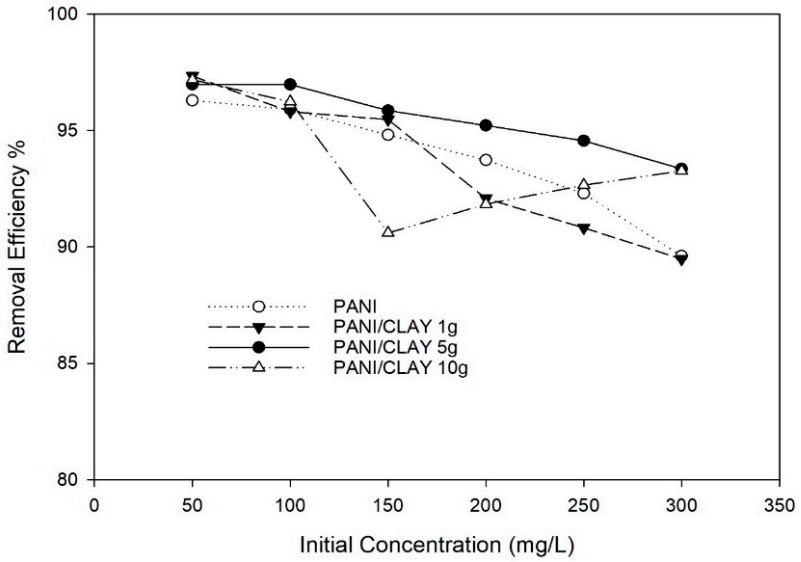


Figure 8. Effect of MO initial concentration on removal efficiency of MO by using prepared adsorbent.

3.2.5. Effect of Temperature

The adsorption % removal efficiency of MO dye increases with temperature, as shown in Figure 9. Increasing the experimental temperature usually leads to an increase in the system's entropy ($\Delta S^\circ > 0$), which in turn leads to more collisions and activities at

the adsorbent–adsorbate interface, thus resulting in higher removal efficiencies. Similar observations were reported for methylene blue adsorption onto mesoporous clay minerals by [48] and for direct blue 106 dye adsorption onto zinc oxide nanoparticles by [49].

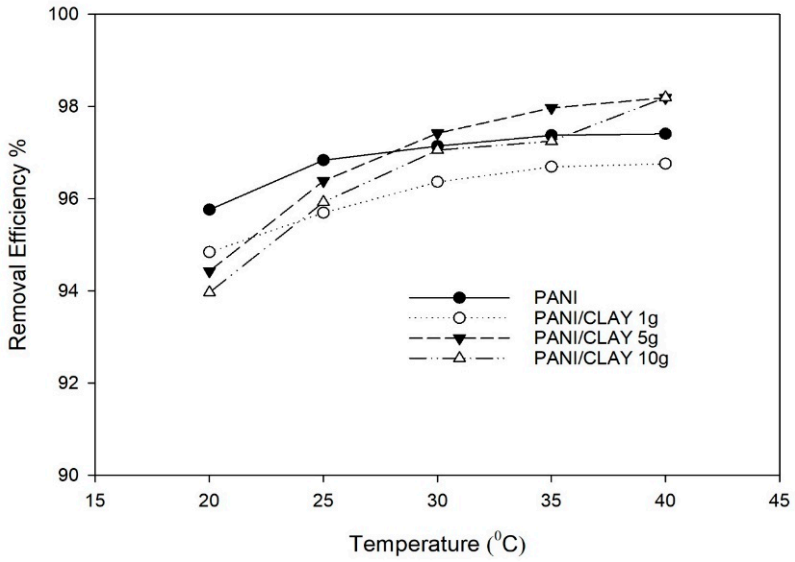


Figure 9. Effect of temperature on removal efficiency of MO by using prepared adsorbent.

3.3. Adsorption Kinetics

Adsorption experiments with respect to contact time were conducted to evaluated the adsorption kinetics and identify the rate limiting step. The quantity of dye adsorbed (q_t) in mg/g at the equilibrium time (t) can be calculated using Equation (3) below:

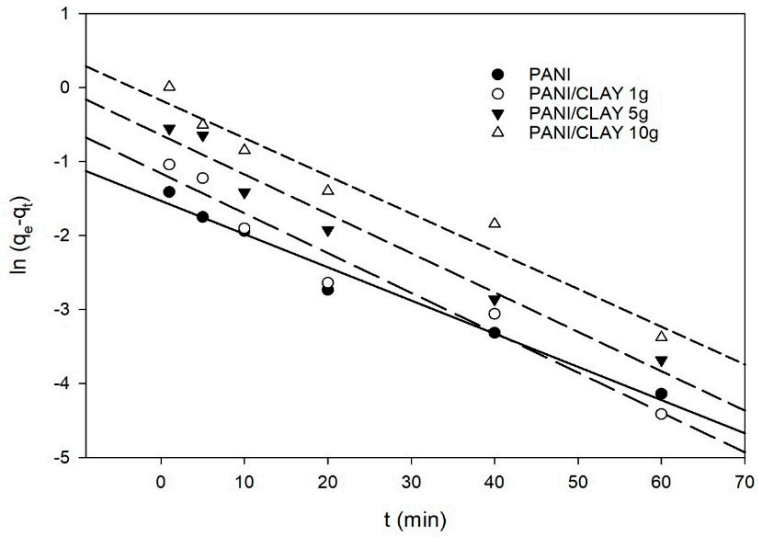
$$q_t = (C_o - C_t)V/W \quad (3)$$

PFO and PSO kinetic models were utilized to gain insight into the regulating mechanism of the adsorption process. They are used to deduce information on the type of interactions (weak or strong) between the adsorbent and adsorbate. Two well-known kinetic models (linearized) are represented by Equations (4) and (5), respectively. A linear plot of $\ln(q_e - q_t)$ against time t for the pseudo-first-order model is illustrated in Figure 10a. Similarly, a linear plot of $\frac{t}{q_t}$ against time t for the pseudo-second-order model is shown in Figure 10b.

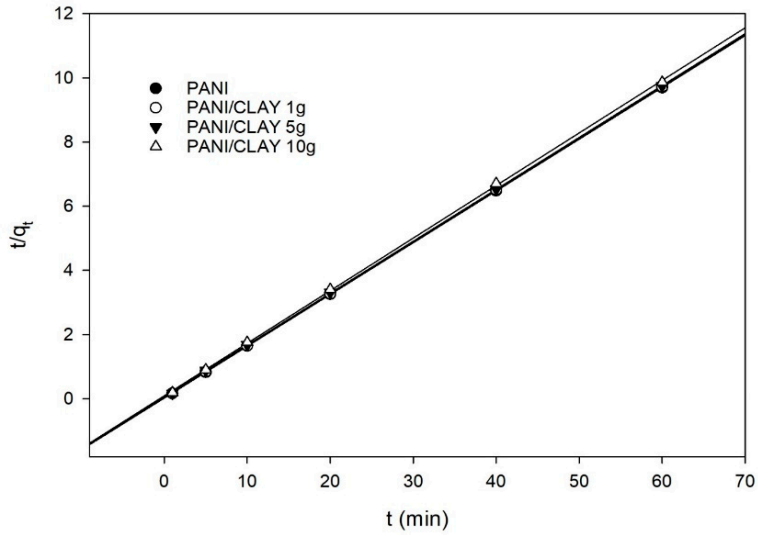
$$\ln(q_e - q_t) = \ln q_e - k_1 t \quad (4)$$

$$\frac{t}{t_q} = \left(\frac{1}{k_2 q_e 2}\right) + \frac{t}{q_e} \quad (5)$$

where C_o is the initial dye concentration (mg/L), C_t is the dye concentration at any time (mg/L), qt is the amount of adsorbed dye at any time, V is the solution volume (L) and W is the adsorbent mass (g). The kinetics data obtained from the graphs for all samples are reported in Table 2. The PSO model fits well the experimental adsorption data, with correlation coefficient R^2 values close to 1, suggesting that MO adsorption on the prepared composites is chemisorption. Furthermore, the pseudo-second-order model showed a good comparison between the predicted and the experimental values of uptake capacity.



(**a**)



(**b**)

Figure 10. Fitting of adsorption kinetics models: (**a**) PFO and (**b**) PSO model.

Table 2. Kinetics data of adsorption of MO onto PANI, PANI/CLAY 1 g, PANI/CLAY 5 g and PANI/CLAY 10 g.

Adsorption Model	Kinetics Parameters	Values			
		PANI	PANI/CLAY 1 g	PANI/CLAY 5 g	PANI/CLAY 10 g
Pseudo-first-order	q_e (mg/g)	0.2168	0.3146	0.5289	0.8452
	k_1 (g/mg/h)	−0.0449	−0.0539	−0.0533	−0.0511
	R^2	0.976	0.9574	0.9707	0.9598
Pseudo-second-order	q_e (mg/g)	6.211	6.196	6.203	6.146
	k_2 (g/mg/h)	0.906	0.704	0.400	0.239
	R^2	1	1	1	0.9999

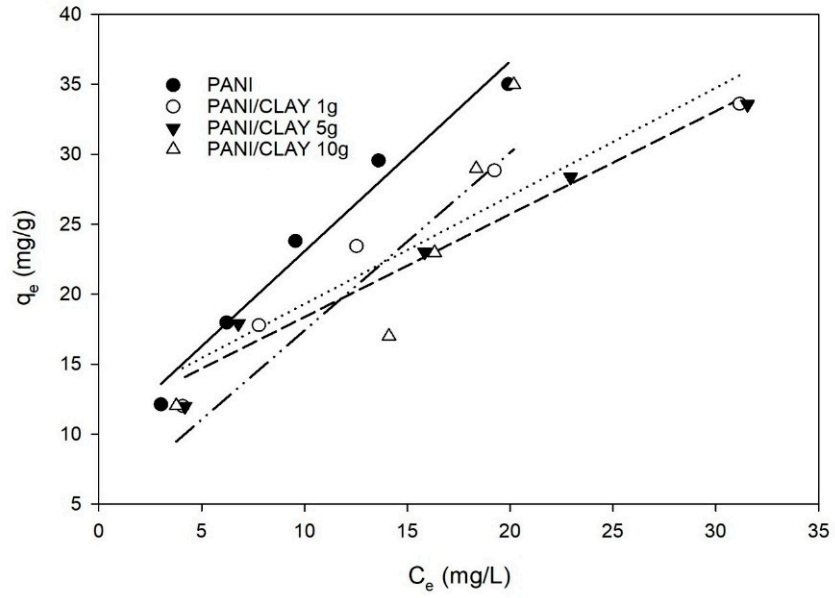
3.4. Adsorption Isotherms

Adsorption isotherm models are commonly applied to understand the type and nature of interactions between the adsorbent and adsorbate. Furthermore, they give information on the best way to explore the nature of adsorbents. Among the different adsorption

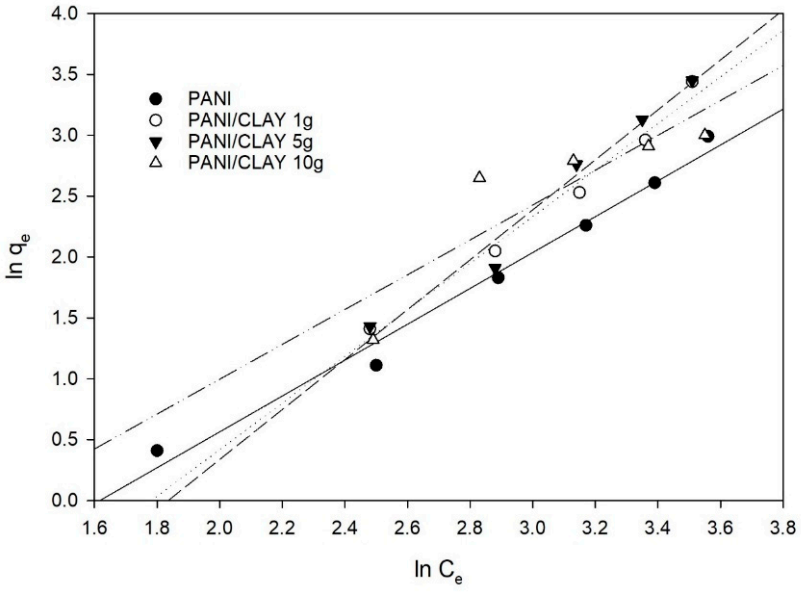
isotherm models, Langmuir, Freundlich and Temkin were used to explore deeper into the interactions that may occur at the adsorbent/adsorbate interface. The linearized Langmuir model is represented by the following equation:

$$\frac{C_e}{q_e} = \frac{1}{K_L q_{max}} + \frac{C_e}{q_{max}} \quad (6)$$

where C_e = equilibrium dye concentration, q_e = uptake capacity and K_L = Langmuir constant. q_{max} refers to the maximum adsorption capacity (mg/g) deduced from the slope and intercept of the plot shown in Figure 11a. To verify the validity of the Langmuir model, (C_e/q_e) was plotted against (C_e), and a straight line was drawn, as shown in Figure 11. Table 3 shows the values of q_{max} and K_L computed from the slope and intercept, respectively.

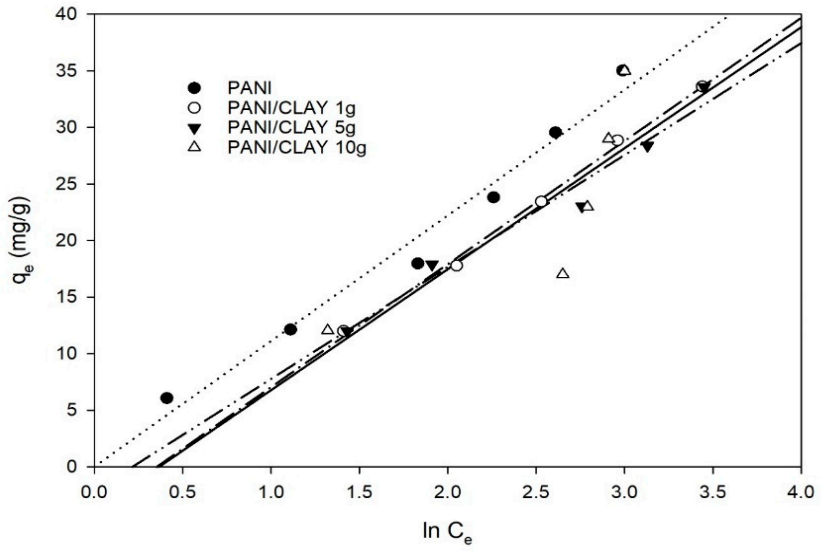


(**a**)



(**b**)

Figure 11. *Cont.*



(**c**)

Figure 11. Adsorption isotherm models fitted to experimental data: (**a**) Langmuir, (**b**) Fruendlich and (**c**) Temkin.

Table 3. Isotherm data of adsorption of MO onto PANI, PANI/CLAY 1 g, PANI/CLAY 5 g and PANI/CLAY 10 g.

Adsorption Isotherm Model	Parameters	Values			
		PANI	PANI/CLAY 1 g	PANI/CLAY 5 g	PANI/CLAY 10 g
Langmuir	q_{max} (mg/g)	55.866	47.170	41.494	42.017
	K_L	0.082	0.080	0.104	0.093
	R^2	0.9873	0.9991	0.9725	0.6496
Freundlich	n	1.502	1.641	1.901	1.762
	1/n	0.6659	0.6093	0.526	0.5675
	K_f	5.155	4.685	5.607	5.112
	R^2	0.9837	0.9754	0.9843	0.9211
Temkin	K_T	1.004	0.874	1.248	1.167
	b_t	223.325	248.306	293.037	283.251
	R^2	0.9784	0.9911	0.9648	0.7813

R_L values are normally calculated using Equation (7) below:

$$R_L = \frac{1}{1 + K_L C_o} \tag{7}$$

where C_o refers to the initial dye concentration. The R_L values can provide information about the type of adsorption, namely favorable, unfavorable and either reversible or irreversible ($0 < R_L < 1$, $R_L > 1$ and $R_L = 0$, respectively). Since the R_L value lies between 0 and 1, favorable adsorption may be deduced.

The Freundlich isotherm model assumes that adsorption site energy distributions decline exponentially. This term is widely used to describe the adsorption properties of a heterogeneous surface. This isotherm also empirically correlates the sorbent's adsorption capacity with its equilibrium constant. Using the following equation, the linearized form of the Freundlich model can be expressed:

$$lnq_e = lnK_f + \frac{1}{n} lnC_e \tag{8}$$

where K_f and n are Freundlich constants. To test the validity of this model, (lnq_e) was plotted against (lnC_e), obtaining a straight line, as shown in Figure 11. K_f and n values were calculated from the slope and intercept, respectively, and are listed in Table 3.

Another important isotherm model is the Temkin model that is linearized and represented by Equation (9) below:

$$q_e = BlnK_T + BlnC_e \quad (9)$$

where B = (R_T/b_t). T is the absolute temperature, R is the universal gas constant, K_T is the Temkin adsorption potential (L/g) and B_T is the Temkin constant, as reported by [50]. The heat of adsorption (J/mol) correlated with b_t was found to be 383.75 J/mol. To illustrate this model, (q_e) was plotted against (lnC_e). From the values of R^2 listed in Table 3, we can say that all three models adequately fit the data to describe the equilibrium of the MO adsorption process.

However, the Freundlich model was found to be a favorable model since the R^2 values are close to 1 for all four composites. The Freundlich equation is used to describe physical adsorption on heterogeneous surfaces. It can be concluded that the experimental data align with the Freundlich isotherm, suggesting that heterogeneous surfaces were utilized. Furthermore, the good fit of the Freundlich model implies that the surface of the adsorbent possesses a range of surface energies. However, the adsorbent's adsorption characteristics are likely to be complicated, suggesting that more than one mechanism may be involved. The 1/n values are between 0 and 1, which demonstrates the greater potential of MO molecules in multilayer adsorption on the active heterogeneous sites of the prepared composites. The adsorption of MO molecules on heterogenous surfaces with a range of surface energies as supported by the good fitting of Freundlich model suggests that the nature of adsorption is physical adsorption.

3.5. Adsorption Thermodynamics

The spontaneity and heat change of the adsorption process were evaluated by carrying out thermodynamic studies, thus allowing us to obtain the thermodynamic parameters, i.e., entropy (ΔS°) changes of adsorption, enthalpy (ΔH°) and free energy (ΔG°). We used the following equations:

$$K_D = \frac{C_0}{C_e} \quad (10)$$

$$\Delta G^\circ = -RT \ln K_D \quad (11)$$

$$\ln K_D = -\frac{\Delta H^\circ}{RT} + \frac{\Delta S^\circ}{R} \quad (12)$$

where K_D is the distribution coefficient of adsorption, C_o (mg L^{-1}) is the initial concentration of the MO solution and C_e (mg L^{-1}) is the equilibrium concentration of the MO solution. T (K) is the absolute temperature, and R is the universal gas constant (8.314 J K^{-1} mol^{-1}). The plot of ln K_D against 1/T as shown in Figure 12 was exploited to determine the values of both ΔH° and ΔS° by using the slope and intercept, respectively. The obtained results are listed in Table 4, which shows that ΔG° values are negative and increase at all the temperatures studied. These negative values of ΔG° demonstrate that the adsorption of MO onto PANI and PANI/CLAY composites is spontaneous and confirms the feasibility of the process [51] since the ΔG° values fall in the range of −20 to 0 kJ/mol. The obtained positive value of ΔH° proves the endothermic nature of the adsorption system. The positive values of ΔS° suggest the increasing randomness at solid/solution interfaces during the adsorption of MO onto adsorbents and reflect the affinity of PANI and PANI/CLAY composites towards MO. Similar results were reported by [52] for fluoride ion adsorption onto

polyaniline/alumina and by [53] for polypyrrole/alumina composites for the elimination of MO as an adsorbate from aqueous solutions.

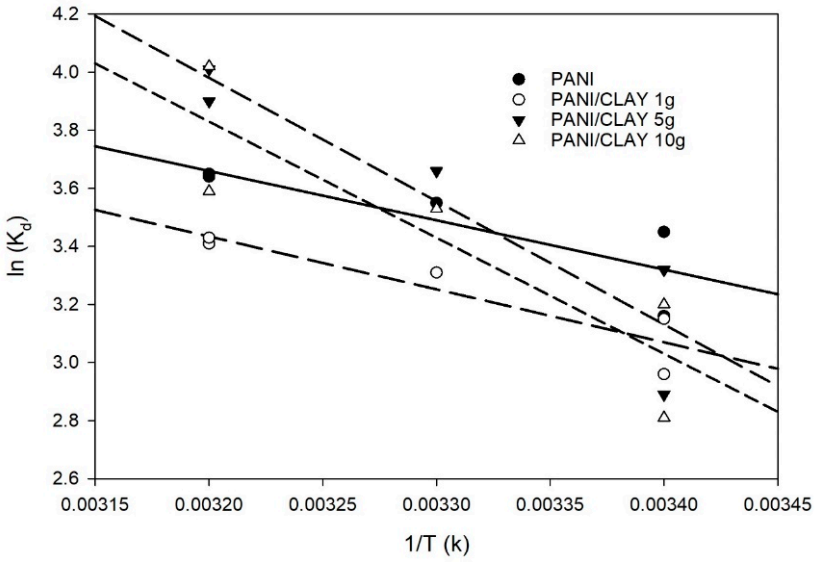


Figure 12. Thermodynamics plots for the removal of MO dye by using the prepared samples.

Table 4. Thermodynamics data of the adsorption of MO onto PANI, PANI/CLAY 1 g, PANI/CLAY 5 g and PANI/CLAY 10 g.

Composite	T (K)	ΔG° (KJ/mol)	ΔH° (KJ/mol)	ΔS° (J/mol K)
PANI	293	−7.70	17.97	88.37
	298	−8.55		
	303	−8.95		
	308	−9.32		
	313	−9.50		
PANI/CLAY 1 g	293	−7.22	18.29	87.42
	298	−7.79		
	303	−8.35		
	308	−8.73		
	313	−8.92		
PANI/CLAY 5 g	293	−7.03	43.31	172.57
	298	−8.23		
	303	−9.21		
	308	−9.98		
	313	−10.45		
PANI/CLAY 10 g	293	−6.84	42.88	170.10
	298	−7.93		
	303	−8.88		
	308	−9.20		
	313	−10.45		

3.6. Comparison of Similar Adsorbents for MO Removal

To assess the suitability of the prepared adsorbents, they were compared with similar adsorbents from the literature on MO removal based on adsorption capacity (mg/g). The adsorbents reported in the current research exhibit relatively attractive and meaningful adsorption characteristics for MO removal compared to other adsorbents for MO removal found in the literature, as shown in Table 5.

Table 5. Comparison of adsorption capacity for MO removal using PANI and PANI/CLAY composites (current research) with different adsorption systems.

Adsorbent	q_{max} (mg/g)	Ref. No.
Halloysite nanoclays	25	[54]
Nanoporous hypercrosslinked polyaniline	220	[55]
Polyaniline nano-adsorbent	75.9	[56]
Immobilized polyaniline glass and polyaniline powder	93 and 147	[29]
Polyaniline $BiVO_4$ nanocomposite	75	[57]
Polyaniline activated carbon composite	285	[30]
Polyaniline nanofibers	25	[38]
Halloysite and chrysotile	13.56 and 31.46	[47]
Polyaniline reinforced activated carbon	46.82 and 192.52	A. Bekhoukh (2022) [58]
Nitrogen-rich polyaniline-based activated carbon	405.6	[59]
Surfactant-modified clay	15.58	[60]
Polyaniline/clay nanocomposite (10 g CLAY, 1 g CLAY and pure PANI)	42.02, 47.17 and 55.87	**This work**

3.7. Possible Removal Mechanism

Methyl orange dye is a polycyclic aromatic compound and therefore can have electron acceptor–donor interactions with the adsorbent. Numerous interactions such as π–π bonding, electrostatic interactions, hydrogen bonding and hydrophobic interactions between the organic dyes and conducting polymers are possible, as reported by [58,61,62]. In most cases of organic dye adsorption, the organic dye becomes attached to the conducting polymer surface through π–π interactions and physicochemical interactions. Furthermore, beside adsorption, dye molecules may be removed by diffusion (absorption) into the phase of the conducting polymer, though the latter process is slower compared to adsorption. The aromatic rings and nitrogen atoms in the polyaniline and MO structure (nitrogen at one end and sodium-substituted sulfur at the other end) are the primary constituents that play a vital role in the interactions. As with clays, MO molecules can be adsorbed by ion exchange [63].

3.8. Reusability Study

Conducting a regeneration and reusability study of an adsorbent is critical since it reveals the socioeconomic and sustainability characteristics of the adsorbent. An adsorption/desorption study was conducted to investigate the reuse possibility of PANI and the PANI/CLAY 5 g composite. To regenerate the adsorbent, sodium hydroxide solution was used followed by rinsing with sulfuric acid. The results of the reusability study are presented in Figure 13. As shown, using the prepared adsorbents PANI and PANI/CLAY 5 g composite, the initial removal efficiency of MO removal was 97% and decreased to 92% for the PANI adsorbent after four cycles. In the case of the PANI/CLAY 5 g composite, no noticeable change was observed in the first three cycles and the removal efficiency decreased from 97% to 96.3% in the fourth cycle. Overall, a small decrease in the removal efficiency % was observed as expected, which is most likely due to a loss of adsorbent during the handling regeneration process. Nonetheless, the investigated adsorbents possess excellent regeneration and reusability characteristics and may be used many times without significant losses in removal efficiency %.

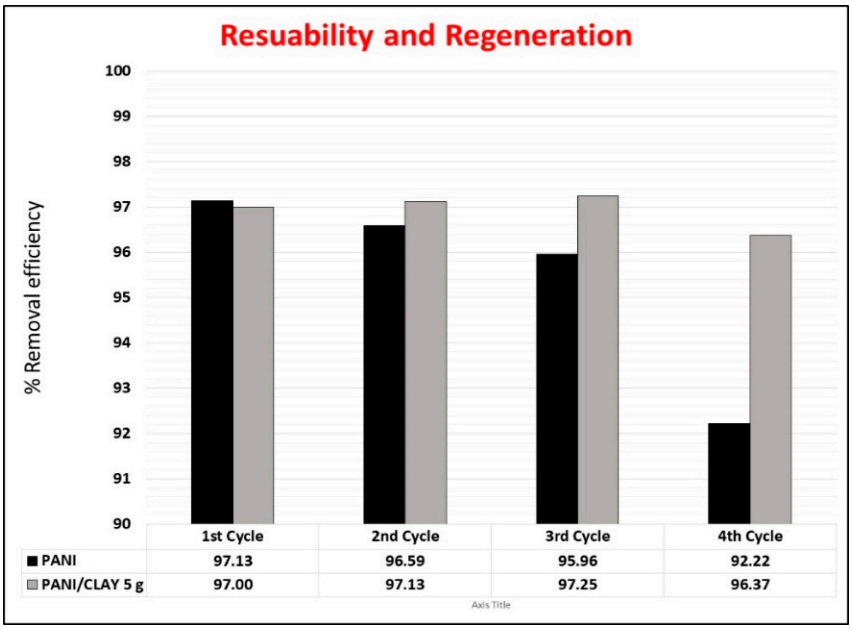


Figure 13. Reusability study for removal of MO dye after 4 cycles.

4. Conclusions

In this study, PANI/clay composites were synthesized and used as adsorbents to remove MO from an aqueous solution under various experimental conditions. The addition of PANI led to a reduction in the specific surface area and pore volume but the maximum uptake capacity increased most likely due to presence of amine and imine functional groups in PANI structure. The TGA results show improved thermal stability of PANI (from 50% weight loss to only 20%) with the clay addition. Optimum removal efficiencies (98–99%) were observed at around a neutral pH value, as confirmed by the pH_{PZC} value. The negative ΔG° values point towards spontaneous adsorption behavior for MO removal by the reported adsorbent material. The maximum uptake capacity q_{max} values were found to increase (42.02, 47.17 and 55.8 mg/g) with increasing PANI contents in the composite. In general, the PANI/clay composites show promising results for the removal of MO even after four cycles.

Author Contributions: Conceptualization, M.I.K. and S.A.Y.; methodology, S.A.Y.; validation, M.I.K., S.A.Y. and I.H.A.; formal analysis, S.A.Y.; investigation, S.A.Y. and A.E.; resources, S.A.Y. and A.E.; data curation, I.S.; writing—original draft preparation, M.I.K. and S.A.Y.; writing—review and editing, I.H.A. and M.R.; visualization, A.M.P.; supervision, M.I.K.; project administration, I.H.A.; funding acquisition, M.I.K. All authors have read and agreed to the published version of the manuscript.

Funding: The authors extend their appreciation to the Deanship of Research and Graduate Studies at King Khalid University, KSA, for funding this work through a large research group under grant number RGP2/533/45.

Data Availability Statement: The original contributions presented in this study are included in the article. Further inquiries can be directed to the corresponding author.

Conflicts of Interest: The authors declare no conflicts of interest.

References

1. Kausar, A.; Iqbal, M.; Javed, A.; Aftab, K.; Nazli, Z.i.H.; Bhatti, H.N.; Nouren, S. Dyes Adsorption Using Clay and Modified Clay: A Review. *J. Mol. Liq.* **2018**, *256*, 395–407. [CrossRef]
2. Hajjaji, M.; Alami, A.; Bouadili, A. El Removal of Methylene Blue from Aqueous Solution by Fibrous Clay Minerals. *J. Hazard. Mater.* **2006**, *135*, 188–192. [CrossRef]

3. Şahin, Ö.; Kaya, M.; Saka, C. Plasma-Surface Modification on Bentonite Clay to Improve the Performance of Adsorption of Methylene Blue. *Appl. Clay Sci.* **2015**, *116–117*, 46–53. [CrossRef]
4. Rauf, M.A.; Salman Ashraf, S. Survey of Recent Trends in Biochemically Assisted Degradation of Dyes. *Chem. Eng. J.* **2012**, *209*, 520–530. [CrossRef]
5. Wang, C.C.; Juang, L.C.; Hsu, T.C.; Lee, C.K.; Lee, J.F.; Huang, F.C. Adsorption of Basic Dyes onto Montmorillonite. *J. Colloid Interface Sci.* **2004**, *273*, 80–86. [CrossRef]
6. Hessel, C.; Allegre, C.; Maisseu, M.; Charbit, F.; Moulin, P. Guidelines and Legislation for Dye House Effluents. *J. Environ. Manag.* **2007**, *83*, 171–180. [CrossRef] [PubMed]
7. Periyasamy, A.P. Recent Advances in the Remediation of Textile-Dye-Containing Wastewater: Prioritizing Human Health and Sustainable Wastewater Treatment. *Sustainability* **2024**, *16*, 495. [CrossRef]
8. Nishino, A.; Taki, A.; Asamoto, H.; Minamisawa, H.; Yamada, K. Kinetic, Isotherm, and Equilibrium Investigation of Cr(VI) Ion Adsorption on Amine-Functionalized Porous Silica Beads. *Polymers* **2022**, *14*, 2104. [CrossRef]
9. Saad, E.M.; Wagdy, M.; Orabi, A.S. Advanced Nano Modification of Ecofriendly Glauconite Clay for High Efficiency Methylene Blue Dye Adsorption. *Sci. Rep.* **2024**, *14*, 23614. [CrossRef]
10. Bhaumik, M.; McCrindle, R.; Maity, A. Efficient Removal of Congo Red from Aqueous Solutions by Adsorption onto Interconnected Polypyrrole-Polyaniline Nanofibres. *Chem. Eng. J.* **2013**, *228*, 506–515. [CrossRef]
11. Chen, H.; Zhao, J.; Zhong, A.; Jin, Y. Removal Capacity and Adsorption Mechanism of Heat-Treated Palygorskite Clay for Methylene Blue. *Chem. Eng. J.* **2011**, *174*, 143–150. [CrossRef]
12. Ighnih, H.; Haounati, R.; Ouachtak, H.; Regti, A.; El Ibrahimi, B.; Hafid, N.; Jada, A.; Labd Taha, M.; Addi, A.A. Efficient Removal of Hazardous Dye from Aqueous Solutions Using Magnetic Kaolinite Nanocomposite: Experimental and Monte Carlo Simulation Studies. *Inorg. Chem. Commun.* **2023**, *153*, 110886. [CrossRef]
13. Ighnih, H.; Haounati, R.; Eshaghi Malekshah, R.; Ouachtak, H.; Toubi, Y.; Alakhras, F.; Jada, A.; Ait Addi, A. Sunlight Driven Photocatalytic Degradation of RhB Dye Using Composite of Bismuth Oxy-Bromide Kaolinite BiOBr@Kaol: Experimental and Molecular Dynamic Simulation Studies. *J. Photochem. Photobiol. A Chem.* **2023**, *445*, 115071. [CrossRef]
14. Liu, P. Polymer Modified Clay Minerals: A Review. *Appl. Clay Sci.* **2007**, *38*, 64–76. [CrossRef]
15. Yagub, M.T.; Sen, T.K.; Afroze, S.; Ang, H.M. Dye and Its Removal from Aqueous Solution by Adsorption: A Review. *Adv. Colloid Interface Sci.* **2014**, *209*, 172–184. [CrossRef]
16. Cottet, L.; Almeida, C.A.P.; Naidek, N.; Viante, M.F.; Lopes, M.C.; Debacher, N.A. Adsorption Characteristics of Montmorillonite Clay Modified with Iron Oxide with Respect to Methylene Blue in Aqueous Media. *Appl. Clay Sci.* **2014**, *95*, 25–31. [CrossRef]
17. Mu, B.; Wang, A. Adsorption of Dyes onto Palygorskite and Its Composites: A Review. *J. Environ. Chem. Eng.* **2016**, *4*, 1274–1294. [CrossRef]
18. Amari, A.; Gannouni, H.; Khan, M.I.; Almesfer, M.K.; Elkhaleefa, A.M.; Gannouni, A. Effect of Structure and Chemical Activation on the Adsorption Properties of Green Clay Minerals for the Removal of Cationic Dye. *Appl. Sci.* **2018**, *8*, 2302. [CrossRef]
19. Pajak, M. Adsorption Capacity of Smectite Clay and Its Thermal and Chemical Modification for Two Anionic Dyes: Comparative Study. *Water. Air. Soil Pollut.* **2021**, *232*, 83. [CrossRef]
20. Xia, H.; Wang, Q. Ultrasonic Irradiation: A Novel Approach To Prepare Conductive Polyaniline/Nanocrystalline Titanium Oxide Composites. *Chem. Mater.* **2002**, *14*, 2158–2165. [CrossRef]
21. Pandiselvi, K.; Thambidurai, S. Chitosan-ZnO/Polyaniline Ternary Nanocomposite for High-Performance Supercapacitor. *Ionics* **2014**, *20*, 551–561. [CrossRef]
22. Mu, B.; Tang, J.; Zhang, L.; Wang, A. Preparation, Characterization and Application on Dye Adsorption of a Well-Defined Two-Dimensional Superparamagnetic Clay/Polyaniline/Fe3O4 Nanocomposite. *Appl. Clay Sci.* **2016**, *132–133*, 7–16. [CrossRef]
23. Nasar, A.; Mashkoor, F. Application of Polyaniline-Based Adsorbents for Dye Removal from Water and Wastewater—A Review. *Environ. Sci. Pollut. Res.* **2019**, *26*, 5333–5356. [CrossRef] [PubMed]
24. Khan, M.I. Adsorption of Methylene Blue onto Natural Saudi Red Clay: Isotherms, Kinetics and Thermodynamic Studies. *Mater. Res. Express* **2020**, *7*, 055507. [CrossRef]
25. Saad, M.; Tahir, H.; Khan, J.; Hameed, U.; Saud, A. Synthesis of Polyaniline Nanoparticles and Their Application for the Removal of Crystal Violet Dye by Ultrasonicated Adsorption Process Based on Response Surface Methodology. *Ultrason. Sonochem.* **2017**, *34*, 600–608. [CrossRef]
26. Lyu, W.; Yu, M.; Feng, J.; Yan, W. Highly Crystalline Polyaniline Nanofibers Coating with Low-Cost Biomass for Easy Separation and High Efficient Removal of Anionic Dye ARG from Aqueous Solution. *Appl. Surf. Sci.* **2018**, *458*, 413–424. [CrossRef]
27. Lyu, W.; Wu, J.; Zhang, W.; Liu, Y.P.; Yu, M.; Zhao, Y.; Feng, J.; Yan, W. Easy Separated 3D Hierarchical Coral-like Magnetic Polyaniline Adsorbent with Enhanced Performance in Adsorption and Reduction of Cr(VI) and Immobilization of Cr(III). *Chem. Eng. J.* **2019**, *363*, 107–119. [CrossRef]

28. Soltani, H.; Belmokhtar, A.; Zeggai, F.Z.; Benyoucef, A.; Bousalem, S.; Bachari, K. Copper(II) Removal from Aqueous Solutions by PANI-Clay Hybrid Material: Fabrication, Characterization, Adsorption and Kinetics Study. *J. Inorg. Organomet. Polym. Mater.* **2019**, *29*, 841–850. [CrossRef]
29. Haitham, K.; Razak, S.; Nawi, M.A. Kinetics and Isotherm Studies of Methyl Orange Adsorption by a Highly Recyclable Immobilized Polyaniline on a Glass Plate. *Arab. J. Chem.* **2019**, *12*, 1595–1606. [CrossRef]
30. Hasan, M.; Rashid, M.M.; Hossain, M.M.; Al Mesfer, M.K.; Arshad, M.; Danish, M.; Lee, M.; El Jery, A.; Kumar, N. Fabrication of Polyaniline/Activated Carbon Composite and Its Testing for Methyl Orange Removal: Optimization, Equilibrium, Isotherm and Kinetic Study. *Polym. Test.* **2019**, *77*, 105909. [CrossRef]
31. Ben Ali, M.; Wang, F.; Boukherroub, R.; Lei, W.; Xia, M. Phytic Acid-Doped Polyaniline Nanofibers-Clay Mineral for Efficient Adsorption of Copper (II) Ions. *J. Colloid Interface Sci.* **2019**, *553*, 688–698. [CrossRef] [PubMed]
32. El-shazly, A.H.; Elkady, M.; Abdelraheem, A. Investigating the Adsorption Behavior of Polyaniline and Its Clay Nanocomposite towards Ammonia Gas. *Polymers* **2022**, *14*, 4533. [CrossRef]
33. Gholami, H.; Shakeri, A.; Saadattalab, V. Investigation of Physical and Mechanical Properties of Polyaniline/MMT Nanocomposites. *Curr. Chem. Lett.* **2017**, *6*, 151–158. [CrossRef]
34. Haloi, D.J.; Ata, S.; Singha, N.K. Synthesis of Poly(2-Ethylhexyl Acrylate)/Clay Nanocomposite via In Situ and Surface Initiated-Atom Transfer Radical Polymerization. *Adv. Sci. Eng. Med.* **2014**, *6*, 240–245. [CrossRef]
35. Majka, T.M.; Leszczyńska, A.; Pielichowski, K. Thermal Stability and Degradation of Polymer Nanocomposites. In *Polymer Nanocomposites*; Springer International Publishing: Cham, Switzerland, 2016; pp. 167–190.
36. Saadattalab, V.; Shakeri, A.; Gholami, H. Effect of CNTs and Nano ZnO on Physical and Mechanical Properties of Polyaniline Composites Applicable in Energy Devices. *Prog. Nat. Sci. Mater. Int.* **2016**, *26*, 517–522. [CrossRef]
37. Panda, A.K.; Mishra, B.G.; Mishra, D.K.; Singh, R.K. Effect of Sulphuric Acid Treatment on the Physico-Chemical Characteristics of Kaolin Clay. *Colloids Surf. A Physicochem. Eng. Asp.* **2010**, *363*, 98–104. [CrossRef]
38. Duhan, M.; Kaur, R. Adsorptive Removal of Methyl Orange with Polyaniline Nanofibers: An Unconventional Adsorbent for Water Treatment. *Environ. Technol.* **2020**, *41*, 2977–2990. [CrossRef]
39. Zhang, S.; Gao, L.; Shan, L.; Wang, R.; Min, Y. Comparative Study on the Adsorption of NO2 Using Different Clay/Polyaniline Composites. *Ind. Eng. Chem. Res.* **2018**, *57*, 6897–6903. [CrossRef]
40. Zhao, W.; Hao, C.; Guo, Y.; Shao, W.; Tian, Y.; Zhao, P. Optimization of Adsorption Conditions Using Response Surface Methodology for Tetracycline Removal by MnFe2O4/Multi-Wall Carbon Nanotubes. *Water* **2023**, *15*, 2392. [CrossRef]
41. Saif Ur Rehman, M.; Munir, M.; Ashfaq, M.; Rashid, N.; Nazar, M.F.; Danish, M.; Han, J.I. Adsorption of Brilliant Green Dye from Aqueous Solution onto Red Clay. *Chem. Eng. J.* **2013**, *228*, 54–62. [CrossRef]
42. Zaremotlagh, S.; Hezarkhani, A. Removal of Textile Dyes from Aqueous Solution by Conducting Polymer Modified Clinoptilolite. *Environ. Earth Sci.* **2014**, *71*, 2999–3006. [CrossRef]
43. Akti, F.; Okur, M. The Removal of Acid Violet 90 from Aqueous Solutions Using PANI and PANI/Clinoptilolite Composites: Isotherm and Kinetics. *J. Polym. Environ.* **2018**, *26*, 4233–4242. [CrossRef]
44. Largo, F.; Haounati, R.; Ouachtak, H.; Hafid, N.; Jada, A.; Addi, A.A. Design of Organically Modified Sepiolite and Its Use as Adsorbent for Hazardous Malachite Green Dye Removal from Water. *Water Air Soil Pollut.* **2023**, *234*, 183. [CrossRef]
45. Deb, A.; Kanmani, M.; Debnath, A.; Bhowmik, K.L.; Saha, B. Ultrasonic Assisted Enhanced Adsorption of Methyl Orange Dye onto Polyaniline Impregnated Zinc Oxide Nanoparticles: Kinetic, Isotherm and Optimization of Process Parameters. *Ultrason. Sonochem.* **2019**, *54*, 290–301. [CrossRef]
46. Ouaddari, H.; Abbou, B.; Lebkiri, I.; Habsaoui, A.; Ouzzine, M.; Fath Allah, R. Removal of Methylene Blue by Adsorption onto Natural and Purified Clays: Kinetic and Thermodynamic Study. *Chem. Phys. Impact* **2024**, *8*, 100405. [CrossRef]
47. Wu, L.; Liu, X.; Lv, G.; Zhu, R.; Tian, L.; Liu, M.; Li, Y.; Rao, W.; Liu, T.; Liao, L. Study on the Adsorption Properties of Methyl Orange by Natural One-Dimensional Nano-Mineral Materials with Different Structures. *Sci. Rep.* **2021**, *11*, 10640. [CrossRef]
48. Auta, M.; Hameed, B.H. Modified Mesoporous Clay Adsorbent for Adsorption Isotherm and Kinetics of Methylene Blue. *Chem. Eng. J.* **2012**, *198–199*, 219–227. [CrossRef]
49. Eleryan, A.; Aigbe, U.O.; Ukhurebor, K.E.; Onyancha, R.B.; Hassaan, M.A. Adsorption of Direct Blue 106 Dye Using Zinc Oxide Nanoparticles Prepared via Green Synthesis Technique. *Environ. Sci. Pollut. Res.* **2023**, *30*, 69666–69682. [CrossRef]
50. Sukla Baidya, K.; Kumar, U. Adsorption of Brilliant Green Dye from Aqueous Solution onto Chemically Modified Areca Nut Husk. *S. Afr. J. Chem. Eng.* **2021**, *35*, 33–43. [CrossRef]
51. Ho, Y.-S. Isotherms for the Sorption of Lead onto Peat: Comparison of Linear and Non-Linear Methods. *Pol. J. Environ. Stud.* **2006**, *15*, 81–86.
52. Karthikeyan, M.; Satheesh Kumar, K.K.; Elango, K.P. Conducting Polymer/Alumina Composites as Viable Adsorbents for the Removal of Fluoride Ions from Aqueous Solution. *J. Fluor. Chem.* **2009**, *130*, 894–901. [CrossRef]
53. Ai, L.; Jiang, J.; Zhang, R. Uniform Polyaniline Microspheres: A Novel Adsorbent for Dye Removal from Aqueous Solution. *Synth. Met.* **2010**, *160*, 762–767. [CrossRef]

54. Chen, H.; Yan, H.; Pei, Z.; Wu, J.; Li, R.; Jin, Y.; Zhao, J. Trapping Characteristic of Halloysite Lumen for Methyl Orange. *Appl. Surf. Sci.* **2015**, *347*, 769–776. [CrossRef]
55. Sharma, V.; Rekha, P.; Mohanty, P. Nanoporous Hypercrosslinked Polyaniline: An Efficient Adsorbent for the Adsorptive Removal of Cationic and Anionic Dyes. *J. Mol. Liq.* **2016**, *222*, 1091–1100. [CrossRef]
56. Tanzifi, M.; Hosseini, S.H.; Kiadehi, A.D.; Olazar, M.; Karimipour, K.; Rezaiemehr, R.; Ali, I. Artificial Neural Network Optimization for Methyl Orange Adsorption onto Polyaniline Nano-Adsorbent: Kinetic, Isotherm and Thermodynamic Studies. *J. Mol. Liq.* **2017**, *244*, 189–200. [CrossRef]
57. Vidya, J.; John Bosco, A.; Haribaaskar, K.; Balamurugan, P. Polyaniline—BiVO4 Nanocomposite as an Efficient Adsorbent for the Removal of Methyl Orange from Aqueous Solution. *Mater. Sci. Semicond. Process.* **2019**, *103*, 104645. [CrossRef]
58. Bekhoukh, A.; Moulefera, I.; Zeggai, F.Z.; Benyoucef, A.; Bachari, K. Anionic Methyl Orange Removal from Aqueous Solutions by Activated Carbon Reinforced Conducting Polyaniline as Adsorbent: Synthesis, Characterization, Adsorption Behavior, Regeneration and Kinetics Study. *J. Polym. Environ.* **2022**, *30*, 886–895. [CrossRef]
59. Al-Odayni, A.B.; Alsubaie, F.S.; Saeed, W.S. Nitrogen-Rich Polyaniline-Based Activated Carbon for Water Treatment: Adsorption Kinetics of Anionic Dye Methyl Orange. *Polymers* **2023**, *15*, 806. [CrossRef]
60. Abbou, B.; Lebkiri, I.; Ouaddari, H.; El Amri, A.; Achibat, F.E.; Kadiri, L.; Ouass, A.; Lebkiri, A.; Rifi, E.H. Improved Removal of Methyl Orange Dye by Adsorption Using Modified Clay: Combined Experimental Study Using Surface Response Methodology. *Inorg. Chem. Commun.* **2023**, *155*, 111127. [CrossRef]
61. Stejskal, J. *Interaction of Conducting Polymers, Polyaniline and Polypyrrole, with Organic Dyes: Polymer Morphology Control, Dye Adsorption and Photocatalytic Decomposition*; Springer International Publishing: Bratislava, Slovakia, 2020; Volume 74, ISBN 0123456789.
62. Stejskal, J. Recent Advances in the Removal of Organic Dyes from Aqueous Media with Conducting Polymers, Polyaniline and Polypyrrole, and Their Composites. *Polymers* **2022**, *14*, 4243. [CrossRef]
63. Iwuozor, K.O.; Ighalo, J.O.; Emenike, E.C.; Ogunfowora, L.A.; Igwegbe, C.A. Adsorption of Methyl Orange: A Review on Adsorbent Performance. *Curr. Res. Green Sustain. Chem.* **2021**, *4*, 100179. [CrossRef]

Disclaimer/Publisher's Note: The statements, opinions and data contained in all publications are solely those of the individual author(s) and contributor(s) and not of MDPI and/or the editor(s). MDPI and/or the editor(s) disclaim responsibility for any injury to people or property resulting from any ideas, methods, instructions or products referred to in the content.